

Thermomechanical behaviour of Steel-Timber Composite beams

Antoine Béreyziat^{a,b}; Maxime Audebert^{c,*}; Sébastien Durif^d; Dhionis Dhima^e and Abdelhamid Bouchaïr^f

ABSTRACT

Full-size Steel Timber Composite (STC) beams, consisting of IPE steel profiles with timber beams embedded between their flanges are tested under four-point bending tests at room temperature and in standard fire conditions (ISO 834 heating curve). The length of the beams is 4.6 m with a load ratio in fire condition set at 43%. The first configuration (STC1) has its bottom flange exposed to fire, while the second (STC2) is fully encapsulated with wider lateral timber beams and a timber element protecting the bottom flange. In normal situation, STC1 and STC2 performed higher strengths than steel profile alone. STC1 and STC2 have a measured fire resistance reaching 29 and 81 min respectively. As a comparison, the estimated fire resistance of an unprotected steel profile is around 13 min. Some temperature measurements show that the deflection of timber and steel elements has an impact on the heat increase of the steel profile. A FEM numerical model is developed and validated on the basis of temperature and deflection measurements. It confirms that timber provides both fire protection and mechanical strengthening for steel in fire conditions.

Keywords: steel; timber; STC beams; fire tests; FEM model.

1. INTRODUCTION

Composite structures aim to get improved performances from complementarities that exists between various materials and components. In this study, it has been chosen to investigate complementarities between hot rolled steel profiles and glulam beams in bending. Previous studies have pointed out that a mutual strengthening can exist if steel and timber are combined in an appropriate way. First, loads are shared between steel and timber according to their respective stiffness when a device (fasteners, glue, contact, etc.) allows loads transfer [1]. Second, in most of existing applications, a steel profile is held laterally by timber members, which increases the buckling resistance [2]. Thus, it is possible to significantly reinforce timber beams using an inlaid steel profile [3] or to strengthen a H steel profile by inserting timber beams between its flanges [4]. Other studies showed that timber components can be used as fire protection for steel profiles. This protection can consist of a timber cladding [5] or a filling of the steel section with timber [6]. This fire protection is already used in Japan for several buildings [7].

^a ENISE, 58 Rue Jean Parot, 42100 Saint-Étienne, France (antoine.bereyziat@enise.fr)

^b ADEME, 20 Avenue du Grésillé, BP 90406, 49004 Angers Cedex 01, France

^{c,*} ENISE, 58 Rue Jean Parot, 42100 Saint-Étienne, France (maxime.audebert@enise.fr)

^d Université Clermont Auvergne, Clermont Auvergne INP, CNRS, Institut Pascal, F-63000 Clermont-Ferrand, France (sebastien.durif@uca.fr).

^e CSTB, 84 Avenue Jean Jaurès, BP 02, 77447 Marne La Vallée Cedex 02, France (dhionis.dhima@cstb.fr).

^f Université Clermont Auvergne, Clermont Auvergne INP, CNRS, Institut Pascal, F-63000 Clermont-Ferrand, France (abdelhamid.bouchaïr@uca.fr).

The goal of this study is to evaluate the behaviour of Steel Timber Composite (STC) beams combining both mechanical and thermal complementarities of the two materials, as highlighted by previous studies. Thus, these hybrid beams could perform higher strength and better fire resistance than those made of a single material. The aim is to better understand the thermomechanical behaviour of such beams using fire tests and numerical simulations.

2. THERMOMECHANICAL TESTS

2.1 Tests description

Figure 1 presents the two configurations STC1 and STC2 that were tested under fire situation. Each configuration has been tested once. These beams consist in IPE 270 steel profiles associated with lateral pieces of glulam (GL24h) embedded between the flanges. The load is shared between timber and steel by contact, no structural shear connection (screws, bolt, etc.) is involved. Thin steel plates are fitted into assembly gaps, between the upper flange of the profile and the timber inner members, to ensure good contact. In the case of STC2 specimen, the timber elements between flanges are wider in order to increase the fire protection and to fix the wooden bottom cover, which is intended to protect the bottom flange of the steel profile from fire. Both configurations have the advantage of providing a mechanical reinforcement of the steel profile. Experimental tests led at room temperature showed an increase of strength, with an improvement of global section strength and also of lateral buckling strength. Indeed, configuration STC1 showed an increase of 38% and STC2 an increase of 68% in strength compared to a single steel profile. Moreover, timber parts protect the steel profile against fire. Configuration STC1 has steel partially exposed to fire, as the bottom flange is non-covered, whereas configuration STC2 offers a full protection against fire.

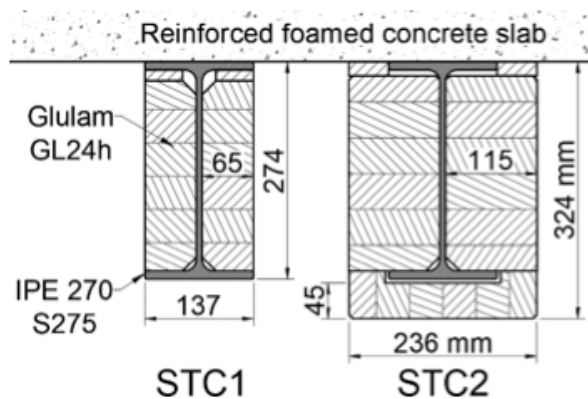


Figure 1: Tested configurations

For each test, a beam with a length of 4.6 m and a span of 4.4 m is exposed to a standard fire, considering the ISO 834 heating curve. The furnace temperature is controlled using 6 plate thermometers during both tests. These temperature measurements inside the furnace show that, after a slightly too high initial heating (between 2 and 3 minutes after the beginning of the test), the heating followed the ISO 834 reference curve with a good accuracy (Figure 4). Figure 2 presents the boundary and loading conditions of the beams, with a constant load in four-point bending test applied on the beams during the heating process. The applied load has been taken as 43% of the average ultimate load-carrying capacity of the beams measured during similar bending tests at room temperature. For each fire test, a 1.0 m long non-loaded beam, similar to the loaded one, is placed into the furnace to evaluate the impact of the loading on the efficiency of the fire protection provided by timber. The instrumentation consists in measuring both displacements and temperatures for the full-scaled beams, and only temperatures for the 1,0 meter non-loaded specimens. The displacements are measured at the mid-span of the beams, as presented in Figure 2.

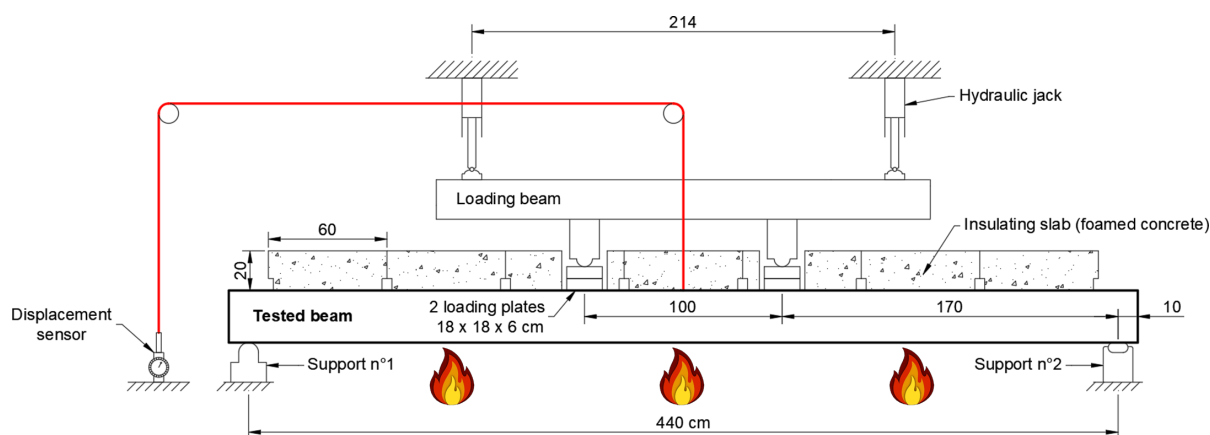


Figure 2: Experimental set-up

Various thermocouples were fitted in the beams in order to measure temperatures on steel and inside timber. In the case of steel temperature, type K thermocouples with a 12 mm diameter copper disc head have been used to measure temperatures along the section height (Figure 3-a). Regarding timber temperatures, type K thermocouples have also been used, with an insulation made of magnesium oxide and an inconel 600 shielding resisting up to 1150°C. Some notches have been made inside timber in order to allow the passage of thermocouples (Figure 3-b). Those thermocouples of 1.5 mm diameter have been inserted through boreholes of 80 mm deep having a 3 mm diameter. Those drilling were made transversally, in the direction parallel to the main exposed surface (lateral face), i.e. parallel to isotherms (Figure 3-c). Previous thermal studies showed that this disposition gives more reliable measurements [8-11].

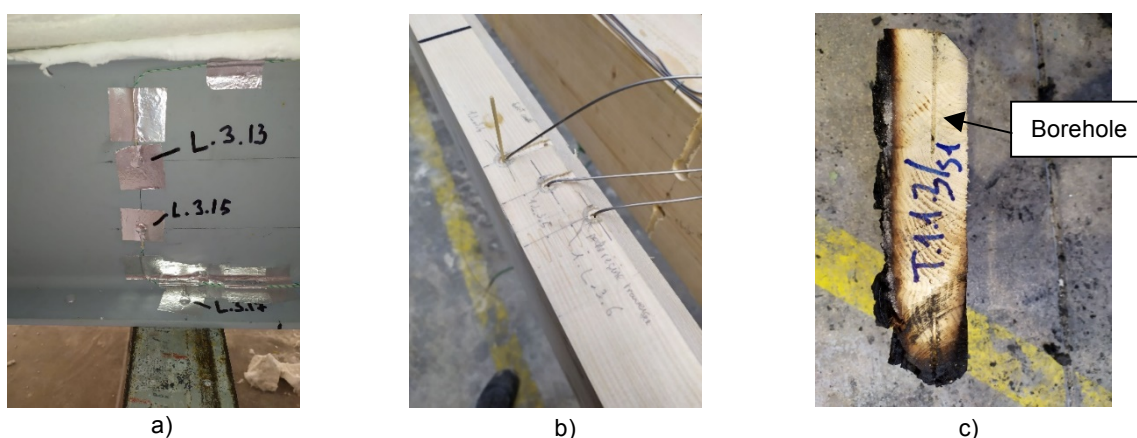


Figure 3: Installation of thermocouples on steel (a) and in timber (b), in boreholes parallel to isotherms (c)

2.2 Test Results

Figure 4 presents the evolution of the mid-span deflection in function of time for both configurations STC1 and STC2. The measured furnace temperatures are also given for both cases and compared to the ISO 834 heating curve. The failure of the beams is determined regarding the deflection value and its acceleration as proposed in EN 1363-1 [12] and EN 13501-2 [13]. For STC1, both criterion (limit deflection and limit deflection rate) are reached. For STC2, the limit deflection value is not reached as the test was stopped due to safety reason. In this case, failure is determined regarding the strain rate only. The load ratio for the test was 43% of the average load-carrying capacity of the beams determined with cold tests. Regarding such ratio, an unprotected steel beam (IPE270) should fail at around 13 min considering an applied calculated bending moment of 66 kN.m. However, it can be observed that the corresponding beam STC1 reaches a failure time of 29 min for an applied bending moment of 91 kN.m. Configuration STC2 reaches a failure time of 81 min for an applied bending moment of 111 kN.m. From those results, it can be said that timber, even only between flanges, provides significantly increased fire resistance.

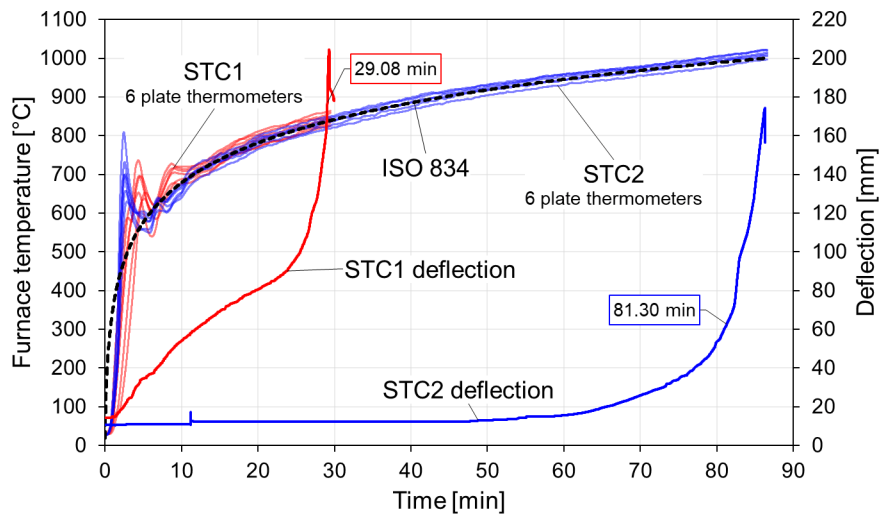


Figure 4: Furnace temperature and mid-span vertical displacement measured for STC1 and STC2

In both cases, timber played a significant role in the fire protection of steel. In the case of STC2, the progressive fall of burnt timber, constituting the protection of the bottom flange, is observed after 72 min of fire exposure. From this point onwards, as the bottom flange of the profile is directly exposed to the fire, the temperatures in the section increase rapidly, leading to the failure of the beam. Figure 5 shows the STC2 beam at the end of the fire test.



Figure 5: Picture of STC2 beam after being extracted from the furnace

The main first result of those test is the impact of the mechanical loading on the temperature increase in the section. Figure 6 compares the temperature of the bottom flange (measuring point n°18) of STC1 at 2 different sections, one located at approximately one fifth of the span and the other located at mid-span. This comparison shows that the exposed flange gets higher temperatures when it is affected by larger vertical displacement. This difference was not observed for the bottom flange when the comparison concerned measured values for non-loaded beam. So, the deflection level has an influence on the temperature of the bottom flange: the deflection induced by the loading tend to increase slightly the bottom flange temperature. In fact, the deflection of the beam induces some local openings of the joint between the bottom flange and the inner timber parts. This clearance is significant when the vertical displacement is important, i.e., at mid-span. We assume that the formation of this gap allows hot gases to heat a larger steel surface, causing the flange to heat up faster. However, in the case of STC1, the temperature difference remains around 50-80°C during the test. The same comparisons can be done for the web temperature (measuring point n°15) as illustrated in Figure 6.

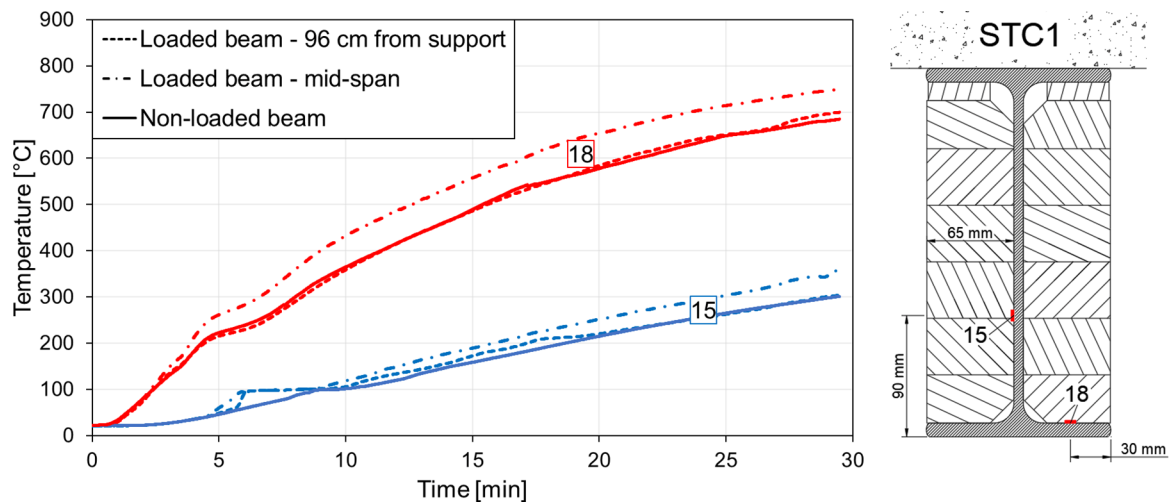


Figure 6: Temperature of the web and the bottom flange of STC1

3. NUMERICAL SIMULATION

3.1 Model Description

A finite element model is developed using the commercial software MSC Marc 2014.2.0 [14]. The thermo-mechanical model is based on an indirect coupling between a thermal model and a mechanical model. The two sub-models are three-dimensional and have strictly similar geometries. A thermal field "mapping" procedure, available in Marc 2014.2, allows considering different meshes for each sub-model. However, the interaction of the mechanical loading on the temperature fields in the materials is neglected: the impact of the beam deflection on the temperatures is not modelled. The mesh is built using hexahedrons-20 nodes elements (HEX20).

Two symmetry planes are considered to optimize the meshed geometry:

- The first one is the symmetry plan of the beam at mid span (figure 7-plane XY). Horizontal longitudinal displacements (along Z axis) are blocked as well as the rotations around X axis.
- The second one is parallel to the beam length (figure 7-plane YZ). It can be considered because geometric instabilities can be neglected. Indeed, the load is too low to induce buckling (43% of the ultimate load), the upper flange is partially connected to the reinforced foamed concrete slab, and the tensile part is the most exposed to fire. So no out-of-plane displacement is expected. Nodes in this plane are blocked from moving in the horizontal-transversal direction (along X axis).

As a result, the modelled geometries correspond to a quarter of the tested beams. Figure 7 gives an overview of the thermomechanical model produced. The load and the support reactions are applied through plates modelled as rigid solids. Contact interactions between solids (timber, steel and loading plates) are achieved by means of "rigid links YY" (Figure 7), i.e., springs that are infinitely rigid in the vertical direction and infinitely flexible in other directions. The fire situation is modelled considering radiative and convective heat flux and the temperature increase follows the average measured furnace temperatures (Figure 4). Radiative and convective parameters are chosen in accordance with Eurocodes [15-17].

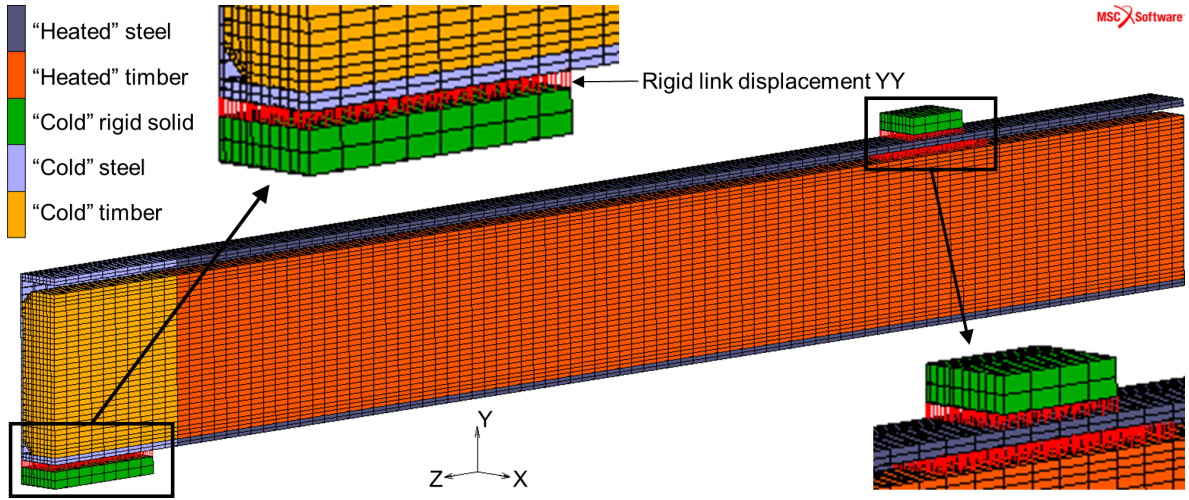


Figure 7: Thermomechanical model for STC1

The elastic limit of steel has been deduced from tensile tests performed on 7 samples [18]. The mean value of the obtained yield limit is 310 MPa. The elastic modulus and the Poisson's ratio are assumed to be 210 GPa and 0.3 respectively, as proposed in EN 1993-1-1 [19]. Steel is modelled as an elastic-perfectly plastic material (bilinear stress-strain curve without hardening).

Timber has been modelled as an anisotropic material, considering a "tetragonal" stiffness matrix [20,21] as described in equation (1). Both, longitudinal elastic modulus (E_L) and bending strength (f_m) have been deduced from bending tests made on 6 full-scale beams (4.6 m long). Three of these beams have dimensions similar to those of the STC1 timber elements, while the other three correspond to the STC2 timber elements (Figure 1). Transversal elastic modulus (E_T) has been deduced from 26 tests made as recommended in EN 408 [22]. The Poisson's ratios (ν_{LT} and ν_{TT}) and shear moduli (G_{LT} and G_{TT}) were deduced from values given by Guitard [23] and according the approach proposed by Davalos et al. [24]. All those values are given in Table 1. The limit of the elastic field is implemented as a Hill criterion and the failure criterion is based on Hoffman [14].

$$\begin{Bmatrix} \epsilon_{11} \\ \epsilon_{22} \\ \epsilon_{33} \\ 2\epsilon_{23} \\ 2\epsilon_{31} \\ 2\epsilon_{12} \end{Bmatrix} = \begin{bmatrix} \frac{1}{E_T} & -\frac{\nu_{TT}}{E_T} & -\frac{\nu_{LT}}{E_T} & 0 & 0 & 0 \\ -\frac{\nu_{TT}}{E_T} & \frac{1}{E_T} & -\frac{\nu_{LT}}{E_T} & 0 & 0 & 0 \\ -\frac{\nu_{LT}}{E_T} & -\frac{\nu_{LT}}{E_T} & \frac{1}{E_L} & 0 & 0 & 0 \\ 0 & 0 & 0 & \frac{1}{G_{LT}} & 0 & 0 \\ 0 & 0 & 0 & 0 & \frac{1}{G_{LT}} & 0 \\ 0 & 0 & 0 & 0 & 0 & \frac{1}{G_{TT}} \end{bmatrix} \begin{Bmatrix} \sigma_{11} \\ \sigma_{22} \\ \sigma_{33} \\ \sigma_{23} \\ \sigma_{31} \\ \sigma_{12} \end{Bmatrix} \quad (1)$$

Table 1: Mechanical properties considered for timber in numerical simulations

Property	STC1	STC2
E_L [MPa]	9 500	11 047
E_T [MPa]	400	400
G_{LT} [MPa]	804	804
G_{TT} [MPa]	84	84
ν_{LT}	0.41	0.41
ν_{TT}	0.41	0.41
f_m [MPa]	29	36

The materials thermophysical and thermomechanical properties are chosen from Eurocodes [16,17] for both steel and timber. However, in the case of timber, some choices have been made by authors, especially regarding the bending strength and the elastic moduli at high temperatures. Indeed, the EN 1995-1-2 proposes reduction factors for either tension or compression [17]. In the current study, the simulated solids are subjected to both tensile and compressive stresses as they are loaded in bending. It has been chosen to manage this issue by using the mean value between tension and compression reduction factors given in EN 1995-1-2, as illustrated in Figure 8.

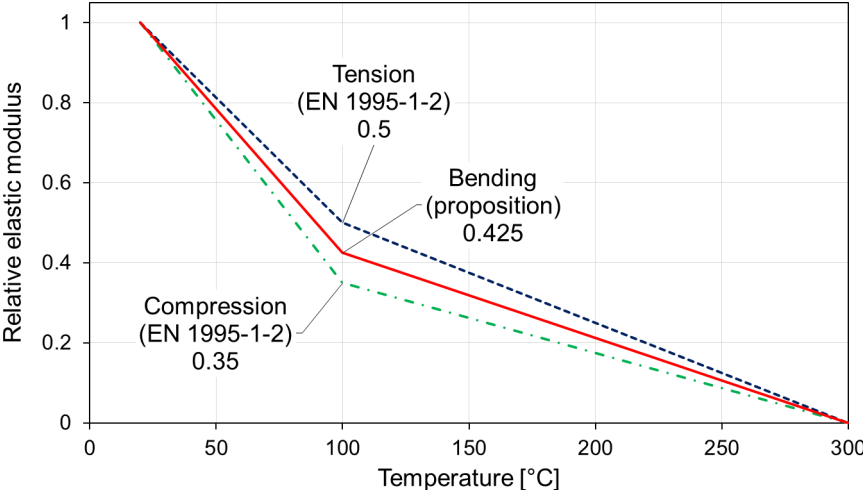


Figure 8: Reduction factors for the elastic moduli of timber.

3.1 Results and discussion

In this section, the results presented for illustration and discussion will be those obtained for the STC1 configuration. Figure 9 presents comparisons between measured and simulated steel temperatures for STC1, considering the unloaded beam. It can be observed that the model agrees well with the experimental results. Some temperature measurement on the web (e.g., measure 16) allow to record a “temperature dwell” around 100°C [25]. It reflects the consequences of the mass transfers that occurs in timber when it is exposed to fire: the accumulation of water against the inner steel parts [26, 27]. This temperature dwell is not reproduced by simulation curves because the dataset used for thermal properties of timber considers mass transfers implicitly [28]. Figure 9 also highlights the heterogeneity of the thermal field across the steel section despite the great thermal conductivity of steel. Even if the lower flange is severely affected by fire, a large part of the web remains at relatively low temperatures.

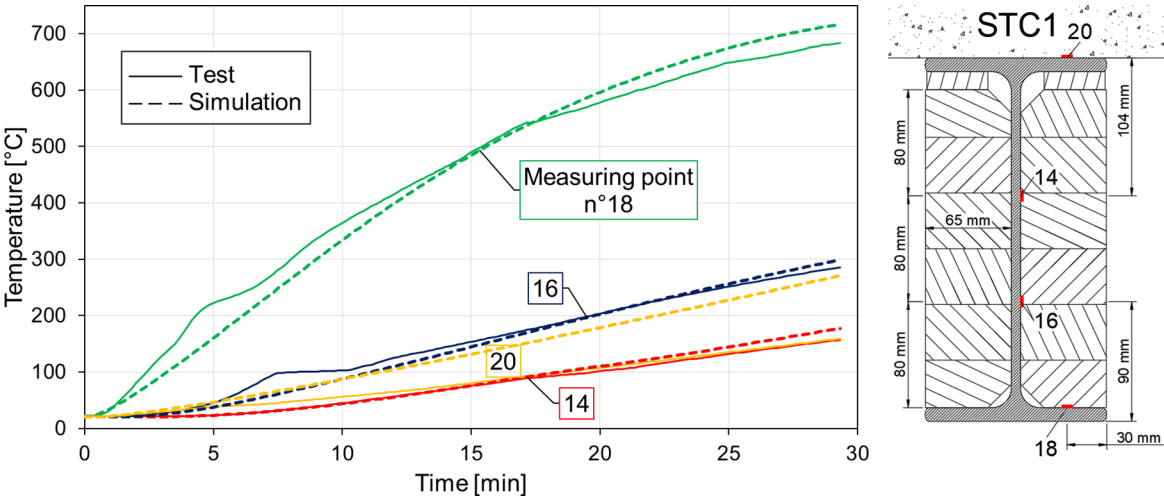


Figure 9: Temperatures on steel for STC1 specimen (non-loaded beam)

Figure 10 shows deflection versus time curves that allow comparison of numerical and experimental results. The numerical model allows to compare the behavior of the beam considering timber just as an insulation material or as a thermomechanical reinforcement, which means that its mechanical properties are also taken in account. It is observed that considering the mechanical strength of timber allows to improve the failure time by 4.7 min (19%). This observation demonstrates that timber contributes to the mechanical response of the beam. This mechanical aspect must be considered with caution as the test conditions, with insulated supports, allows a good transfer of force between steel and timber. It may be different in the case of a totally exposed beam and be more dependent on the connection device between steel and timber.

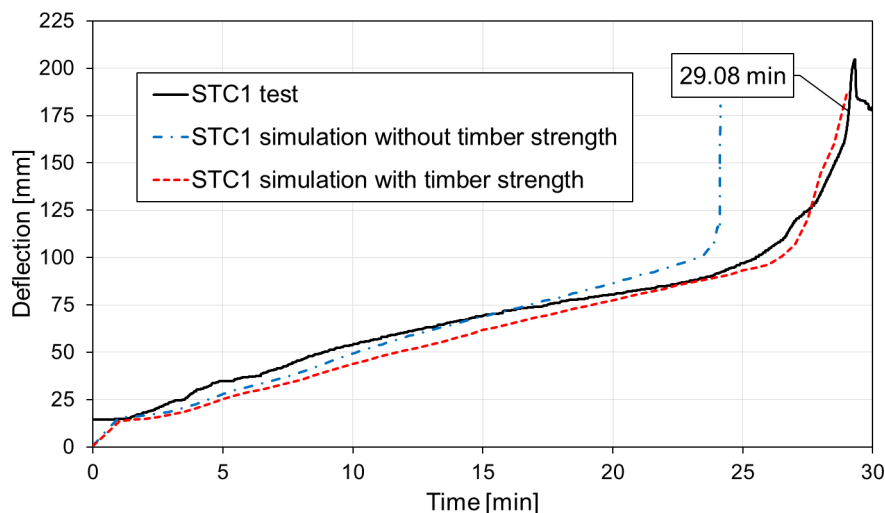


Figure 10: Mid-span vertical displacement of STC1 during fire exposure

4. CONCLUSIONS

The conducted fire tests showed that STC beams have a twofold benefit:

- There is a mutual reinforcement of steel and timber. This mutual strengthening allows configuration STC1 to bear a load 1.38 times greater than the one that an IPE270 steel profile can support. This ratio increases to 1.68 for STC2.
- Timber provides fire protection for steel and delays its collapse by taking up more load as the strength of steel decreases. An unprotected IPE270 steel profile has a fire resistance of 13 min when a 43% load ratio is considered, while STC1 and STC2 withstand fire conditions for 29 min and 81 min respectively under the same load level.

Some temperature measurement showed that the mechanical load impacts the thermal behaviour by deforming steel and timber in a different way, resulting in an opening of assembly joints. These clearances conduct timber to burn faster and steel to heat up more rapidly as it becomes more exposed to fire. Increasing the sinuosity of the assembly joints or keeping them closed (e.g., using glue) could result in better fire resistance.

Tests also allowed to point out that the char fall-off is of major importance in the case of fully protected configurations (like STC2). In this study, the solution chosen to protect the bottom flange is to fasten a machined timber protection on it using screws, but many other possibilities exist. The fire behaviour and the char fall-off may vary depending on the selected technical choice, so more experimental investigations may be needed.

The FEM simulation approach using the datasets proposed in Eurocodes [15-17] is found to give results in good agreement with temperature measurements in both timber and steel. The adjustment of reduction factors given in EN 1995-1-2 [17] to suit the case of a bending load is found to be satisfactory. Simulations based on the STC1 configuration showed that timber improve the fire resistance of steel profile by means of two mechanisms: it acts as a fire protective material, and it provides mechanical reinforcement by taking up the load that steel can no longer withstand as its mechanical properties decrease under the effect of heat. The simulation of the STC2 configuration is of less interest as the char fall-off is difficult to predict, resulting in less accurate results.

Therefore, simplified rules for fire-design, e.g., like the one proposed by Riola Parada [1], could be a suitable approach for this kind of STC beam.

5. ACKNOWLEDGEMENTS

Authors thank the Scientific and Technical Centre for Building (CSTB) and the Environmental and Energy Management Agency (ADEME) for funding this work. Authors thank the following companies for providing timber and steel: Gagne construction métallique, Coladello and MECD for their contribution.

6. REFERENCES

- [1] Riola Parada, F. (2016). *Timber-steel Hybrid beams for multi-storey buildings*, PhD Thesis, Technischen Universität Wien, 245 p.
- [2] Jurkiewicz, B.; Durif, S.; Bouchaïr, A. & Grazide, C. (2022). *Experimental and analytical study of hybrid steel-timber beams in bending*, *Structures*, vol. 39, p. 1231–1248. doi: 10.1016/j.istruc.2022.03.055.
- [3] Fujita, M. & lwata, M. (2013). *Bending test of the composite steel-timber beam*, *Appl. Mech. Mater.*, vol. 351–352, p. 415–421. doi: 10.4028/www.scientific.net/AMM.351-352.415.
- [4] Duan, S.; Zhou, W.; Liu, X.; Yuan, J. & Wang, Z. (2021). *Experimental Study on the Bending Behavior of Steel-Wood Composite Beams*, *Adv. Civ. Eng.*, vol. 2021, p. 1315849. doi: 10.1155/2021/1315849.
- [5] Twilt, L. & Witteveen, J. (1974). *The fire resistance of wood-clad steel columns*, *Fire Prev. Sci. Technol.*, vol. 11, p. 14–20.
- [6] Masuda, H.; Yusa, S.; Kawai, T. & Namiki, Y. (2004). *Fire resistance of hybrid wooden structure, Part 9: Loaded fire resistance test on heavy-timber beam structure*, Annual meeting of Architectural Institute of Japan, p. 139–140.
- [7] JR East Design Corporation (2016). *Kunimi Town Office Building, Steel construction Today & Tomorrow*, no. 49, p. 15–18.
- [8] Beck, J. V. (1962). *Thermocouple temperature disturbances in low conductivity materials*, *J. Heat Transfer*, vol. 84, no. 2, p. 124–131. doi: 10.1115/1.3684310.
- [9] Fahrni, R.; Schmid, J.; Klippel, M. & Frangi, A. (2018). *Correct temperature measurements in fire exposed wood*, World Conference on Timber Engineering, 10 p. doi: 10.3929/ethz-b-000289850.
- [10] Terrei, L.; Acem, Z.; Marchetti, V.; Lardet, P.; Boulet, P. & Parent, G. (2021). *In-depth wood temperature measurement using embedded thin wire thermocouples in cone calorimeter tests*, *Int. J. Therm. Sci.*, vol. 162, 11 p. doi: 10.1016/j.ijthermalsci.2020.106686.
- [11] Nguyen, M. H.; Ouldboukhitine, S. E.; Durif, S.; Saulnier, V. & Bouchaïr, A. (2023). *Method of measuring the temperature of wood exposed to fire with type K thermocouples*, *Fire Saf. J.*, vol. 137, p. 103752. doi: <https://doi.org/10.1016/j.firesaf.2023.103752>.
- [12] European Committee for Standardization (2020). *EN 1363-1 - Fire resistance tests - Part 1: general requirements*.
- [13] European Committee for Standardization (2016). *EN 13501-2 - Fire classification of construction products and building elements - Part 2: classification using data from fire resistance tests, excluding ventilation services*.
- [14] MSC Software Corporation (2015). *Marc 2014.2 - Volume A: Theory and User Information*.
- [15] European Committee for Standardization (2002). *EN 1991-1-2 - Eurocode 1 - Actions on structures – Part 1-2: General actions - Actions on structures exposed to fire*.
- [16] European Committee for Standardization (2005). *EN 1993-1-2 - Eurocode 3 - Design of steel structures - Part 1-2: General rules - Structural fire design*.
- [17] European Committee for Standardization (2004). *EN 1995-1-2 - Eurocode 5 - Design of timber structures - Part 1-2: General - Structural fire design*.
- [18] European Committee for Standardization (2019). *EN ISO 6892-1 - Metallic materials - Tensile testing - Part 1: method of test at room temperature*.
- [19] European Committee for Standardization (2005). *EN 1993-1-1 - Eurocode 3 - Design of steel structures - Part 1-1 : General rules and rules for buildings*.
- [20] Dieulesaint, E. & Royer, D. (1974). *Ondes élastiques dans les solides: application au traitement du signal*, Masson, 399 p.
- [21] Lemaitre, J. ; Chaboche, J. L.; Benallal, A. & Desmorat, R. (2020). *Mécanique des matériaux solides*,

- Dunod, 596 p.
- [22] European Committee for Standardization (2012). *EN 408+A1 - Structural timber and glued laminated timber - Determination of some physical and mechanical properties*.
 - [23] Guitard, D. (1987). *Mécanique du matériau bois et composites*, Cépaduès, 238 p.
 - [24] Davalos, J. F.; Loferski, J. R.; Holzer, S. M. & Yadama, V. (1991). *Transverse Isotropy Modeling of 3-D Glulam Timber Beams*, *J. Mater. Civ. Eng.*, vol. 3, no. 2, p. 125–139. doi: 10.1061/(ASCE)0899-1561(1991)3:2(125).
 - [25] White, R. H. & Schaffer, E. L. (1981). *Transient Moisture Gradient in Fire-Exposed Wood Slab*, *Wood Fiber Sci.*, vol. 13, no. 1, p. 17–38.
 - [26] Audebert, M.; Dhima, D.; Taazount, M. & Bouchaïr, A. (2014). *Experimental and numerical analysis of timber connections in tension perpendicular to grain in fire*, *Fire Saf. J.*, vol. 63, p. 125–137. doi: 10.1016/j.firesaf.2013.11.011.
 - [27] Sedighi Gilani, M.; Hugi, E.; Carl, S.; Palma, P. & Vontobel, P. (2015). *Heat Induced Desorption of Moisture in Timber Joints with Fastener During Charring*, *Fire Technol.*, vol. 51, no. 6, p. 1433–1445. doi: 10.1007/s10694-014-0416-3.
 - [28] König, J. (2006). *Effective thermal actions and thermal properties of timber members in natural fires*, *Fire Mater.*, vol. 30, no. 1, p. 51–63. doi: 10.1002/fam.898.